crystals

MDPI

Article

Effect of Liquid Crystalline Acrylates on the Electro-Optical Properties and Micro-Structures of Polymer-Dispersed Liquid Crystal Films

Cong Ma [1], Yishuo Wu [2], Meina Yu [2], Yanzi Gao [2], Jiumei Xiao [3], Cheng Zou [2,*] and Huai Yang [1,*]

[1] School of Materials Science and Engineering, Peking University, Beijing 100083, China
[2] Institute for Advanced Materials and Technology, University of Science and Technology Beijing, Beijing 100083, China
[3] School of Mathematics and Physics, University of Science and Technology Beijing, Beijing 100083, China
* Correspondence: zoucheng@ustb.edu.cn (C.Z.); yanghuai@pku.edu.cn (H.Y.)

Abstract: Polymer-dispersed liquid-crystal (PDLC) films have wide applications in light shutters, smart windows for cars and buildings, dimming glasses, and smart peep-proof films due to their switchable optical states under electrical fields as well as large area processibility. They are usually prepared with liquid crystals (LCs) and non-liquid crystalline monomers (NLCMs). Introduction of liquid crystalline monomers (LCMs) into PDLCs might spark new functionality or high-performance devices such as polymer-dispersed and -stabilized liquid crystals. In this study, the effect of molecular structures and doping concentrations of acrylate LCMs on the electro-optical properties and micro-structures of PDLC films is systematically studied. The pore size of polymer networks and the driving voltage of the PDLC films are affected by the molecular polarity and degree of functionality of the LCMs. The electro-optical properties of the PDLC films are affected by the synergistic influence of molecular structure of LCMs and micro-structures of PDLCs. These results might provide the experimental and theoretical basis for constructing the relationship between the molecular structure of LCM, micro-structure and electro-optical response of PDLC films.

Keywords: liquid crystalline monomers; acrylates; polymer-dispersed liquid crystals; electro-optical properties; micro-structure

check for updates

Citation: Ma, C.; Wu, Y.; Yu, M.; Gao, Y.; Xiao, J.; Zou, C.; Yang, H. Effect of Liquid Crystalline Acrylates on the Electro-Optical Properties and Micro-Structures of Polymer-Dispersed Liquid Crystal Films. *Crystals* **2023**, *13*, 1294. https://doi.org/10.3390/cryst13091294

Academic Editor: Pedro De Almeida

Received: 7 August 2023
Revised: 19 August 2023
Accepted: 20 August 2023
Published: 22 August 2023

Copyright: © 2023 by the authors. Licensee MDPI, Basel, Switzerland. This article is an open access article distributed under the terms and conditions of the Creative Commons Attribution (CC BY) license (https://creativecommons.org/licenses/by/4.0/).

1. Introduction

Climate challenges and the energy crisis are the most crucial problems faced by our society. Transportation and building energy consumption account for the majority of total energy consumption [1]. To bring down the growing energy consumption, there is an urgent need to design efficient and low-cost smart windows to block the superfluous solar energy [2]. Polymer-dispersed liquid crystal (PDLC) films are a promising candidate for smart windows, which possess excellent mechanical properties and switchable optical properties under electrical fields. Due to their high polymer content (ca. $\geq$ 40.0 wt%), large-area flexible PDLC films could be fabricated through roll-to-roll process, which could realize low-cost, high-efficiency industrial production [3–6]. A good PDLC device embraces all these advantages, such as low switching voltage, quick response time, high contrast ratio, and high stability and safety [7–10]. Due to the electro-optical switching capabilities of PDLC films, they can also be used as a display material [11–14].

In PDLC films, liquid crystals (LCs) are encapsulated in the polymer matrix in the form of droplets. The principles of its light control are as follows: when the electric field is off, due to the random distribution of directors of LCs, there exists a difference between the refractive index of LC droplets and that of the polymer matrix, making the PDLC films present a strong light-scattering state. After applying an electric field of certain intensity across the LC cells, since LC materials with positive dielectric anisotropy are generally used

in PDLC films, the directors of LCs are rearranged along the direction of the electric field, re-matching the refractive index of LC droplets with that of the polymer matrix and making the PDLC films present a transparent state. As a result, reversible switching between transparent state and scattering state can be achieved through consecutive adjustments of light control by altering the direction of LC droplets with an electric field [15–17].

However, PDLC films often suffer from problems such as high driving voltage, haze change at different viewing-angles, and limited functions, which impede their application in cars and buildings. In previous studies, most researchers focused on optimizing the performances of PDLCs by introducing different nanoparticles or non-liquid crystalline monomers (NLCMs). Jia considered high electro-optical performance can be realized with the introduction of TiO_2 nanoparticles [18]. Yu thought hydroxylated acrylate monomer was of significance for improving electro-optical properties of the PDLC films [19]. Zhang reduced the brittleness of PDLC devices using a novel type of silver nanowires [20]. Jamil M. realized quicker response time and lower haze by doping nanomaterials [21]. Kizhakidathazhath discovered a low-voltage driven PDLC system containing acrylate monomer (A3DA) characterized by a benzene moiety with a dodecyl terminal chain [22]. Ghosh realized energy saving through sandwiching PDLC glazing between a vacuum and one acrylic sheet (Vacuum-PDLCA) and vacuum and glass (Vacuum-PDLCG) [23]. Bobnar and his co-workers devised a shape-memory composite material that was based on PDLC elastomers and can be made effortlessly and effectively [24]. Yu achieved the decrease in both driving voltage and hysteresis by doping acrylate NLCMs with different steric end groups into PDLC devices [25]. In recent studies, researchers started to focus on the introduction of LCMs into PDLC. Acrylate LCM is a type of monomer which has both rigid mesogen and flexible alkyl chain, whose polymerization rate is relatively lower than NLCM due to the lower chance of collision between molecules. Guo suggested an electrical light transmittance-controllable PDLC film that featured lower driving voltage by step-polymerization using NLCMs and LCMs as monomers [26]. Liang proposed a new procedure to fabricate a flexible multi-responsive smart film in which the polymer matrix and polymer networks co-exist via polymerization of NLCMs at first and polymerization of LCMs afterwards. By adjusting temperature and electric field, flexibility and safety can be achieved through the introduction of LC polymerizable monomers [27,28]. Although the introduction of LCM into PDLC could endow PDLC with new functionality or high-performance, the effect of LCM on the PDLC is still unclear.

Herein, a series of liquid crystalline monomers with acrylate end groups were introduced into the PDLC film to study the effect of LCMs on the electro-optical properties and micro-structures of PDLC films. The influence of molecular structure and content of LCMs on the PDLC films were systematically studied. The driving voltage and pore size of PDLC films were found to be greatly affected by the molecular polarity and degree of functionality of the LCMs. The study might provide an experimental and theoretical basis for establishing the relationship between molecular structure, micro-structure, and electro-optical performance of PDLC films.

2. Materials and Methods

Materials: The materials used in this study include LC mixture, photo-polymerizable monomers, and photo initiator (Irgacure 651). The nematic LC: SLC1717 (birefringence $\Delta n = 0.201$, extraordinary refractive index $n_e = 1.720$, phase transition temperature from crystallization (Cr) to nematic (N) phase $T_{Cr\text{-}N} < -20\ ^{\circ}C$) was purchased from Yantai Xian Hua Chem Tech. Co., Ltd., Yantai, China. NLCM: 3,5,5-trimethylhexyl acrylate (TMHA), 1,4-butanediol diacrylate (BDDA), were obtained from Aladdin Industrial Inc., Shanghai, China. LCM: Cyano mono-acrylate monomer (CN), carboxyl mono-acrylate monomer (C6A), and methoxyl mono-acrylate monomer (OMe) were purchased from Jiangsu Hecheng Advanced Material Co., Ltd., Nanjing, China. Irgacure 651 (IR651) was purchased from Bide Pharmatech Ltd. (Shanghai, China).

Preparation of PDLC devices: The photopolymerizable NLC monomers and LC monomers with nematic LC and IR651 were mixed at 353.15 K according to the ratios in Table S1. After mixing with vibration stirring for 10 min, the mixture formed a homogeneous solution and was filled into an LC cell with 20 μm gap through capillary action at 353.15 K. After keeping the samples at the temperature of 353.15 K for 5 min, the samples were cooled to room temperature. Subsequently, the samples were photo-polymerized under 365 nm UV light with light intensities of 25 mW/cm^2 for 300 s at room temperature by UV lamp (XM210 UVLED purchased from Aventk, Shanghai, China).

Measurements of Polymer Network Morphology: A scanning electron microscope (SEM, JSM-6700F, Tokyo, Japan) was used to characterize the morphology of the polymer networks. To obtain its top-view images, the samples were firstly soaked in cyclohexane at room temperature for 3 days to remove the nematic LC molecules and retained samples only containing the polymer network. Then, they were cut off in middle sections. The polymer network morphology can be observed under SEM after the samples were sprayed with gold.

Measurements of electro-optical performance of the PDLC devices: The PDLC devices were driven by 100 Hz sinusoidal AC, and a transformer was used to change the applied voltage. Transmittance, contrast ratio, threshold voltage, saturation voltage, and response time of the PDLC devices were all tested by a LCD comprehensive parameter meter (LCT-5066C; The North LCD Engineering R&D Center, Changchun, China). The transmittance is normalized by measuring the transmittance of a standard empty LC cell, each component is tested with at least three samples.

3. Results and Discussion

3.1. Effect of Temperature and UV Intensity on the Electro-Optical Performance of PDLC

In traditional PDLC films prepared with non-liquid crystalline monomers (NLCMs), it is of vital importance to maintain a suitable ultraviolet (UV) intensity and polymerization temperature for the preparation of devices that have optimized electro-optical performance. As a result, temperature of polymerization was researched before the introduction of LCMs. Temperature of polymerization mainly exerts an influence on the reaction rate of photopolymerization, further affecting the micro-structure and mechanical property of polymer network. The clearing point of pre-polymerized NLCM and LC mixtures were firstly tested. It can be seen from Figure S1 that in the range of 5.0–35.0 °C under polarized optical microscope, with the temperature increasing, the state of mixtures has changed from liquid crystal phase to isotropic phase. When the temperature reaches 30.0 °C, the state of mixtures became liquid with isotropic phase. The polymerization temperature was set at 25.0 °C, 35.0 °C, 45.0 °C, 55.0 °C, and 65.0 °C, respectively. Electro-optical performance of the PDLCs prepared at different temperature was shown in Figure 1. When the temperature of polymerization remains under 35.0 °C, both threshold voltage (V_{th}) and saturation voltage (V_{sat}) maintained at a lower level, that is, V_{th} fluctuates at 5.0 V and V_{sat} is slightly higher than 10.0 V. In contrast, when the temperature of polymerization was higher than 35.0 °C, V_{th} increased a bit while V_{sat} increased sharply. It indicates that with the increase in the polymerization temperature, stronger anchoring action of PDLC networks on LCs results in higher voltage for LCs to drive. The Sample T1 prepared at 25.0 °C showed the best contrast ratio and response time. This was consistent with other research that preparation temperatures for samples with optimized electro-optical performances basically remain at 5.0 °C below the clear point. So, to obtain optimal electro-optical performance of PDLC films in this study, the polymerization temperature was set at 25.0 °C.

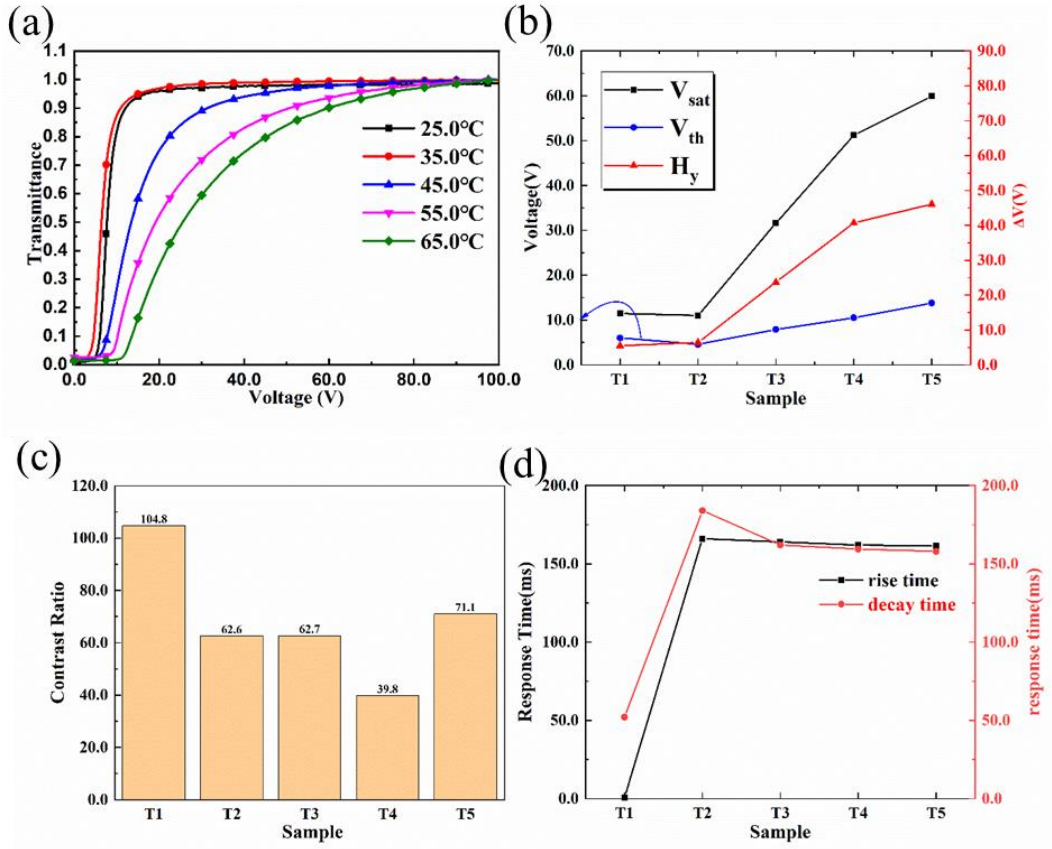


Figure 1. Electro-optical performance curves of PDLC films prepared at different temperatures from 25.0 °C to 65.0 °C. (**a**) Voltage–transmittance curves; (**b**) threshold voltages, saturation voltages and difference between them from Sample T1 to Sample T5; (**c**) contrast ratios from Sample T1 to Sample T5; (**d**) rise times and decay times from Sample T1 to Sample T5.

After ensuring the polymerization temperature remained at 25.0 °C, the influence of UV intensity on electro-optical performance of PDLC films was studied. UV intensity mainly affects the reaction rate of NLCMs' photopolymerization, thus influencing the topology and mechanical properties of polymer networks. Therefore, it is necessary to determine the appropriate UV intensity for the follow-up research. Samples with a composition the same as N0-1 were prepared at a polymerization temperature of 25.0 °C under different UV intensities (5.0–35.0 mW/cm^2). As shown in Figure 2, the voltage–transmittance curves of samples under various UV light conditions have little difference. For the initial transmittance, the sample under the condition of UV intensity of 25.0 mW/cm^2 was the lowest, which was 50.0% lower than that of the sample with the highest initial transmittance. The contrast of Sample U3 also remained highest in contrast curves, 1.2 to 2.4 times that of other samples under other conditions. In terms of voltage curves and response time curves, compared with samples under other UV intensities, Sample U3 had a lower voltage and a quicker response time. The above curves of electro-optical performances show that the PDLC device with a UV intensity of 25.0 mW/cm^2 has the best electro-optical properties. In studies of the temperature of polymerization and UV intensity required for polymerization, the best preparation condition of PDLC devices containing NLCMs only is a polymerization temperature of 25.0 °C with a UV intensity of 25.0 mW/cm^2.

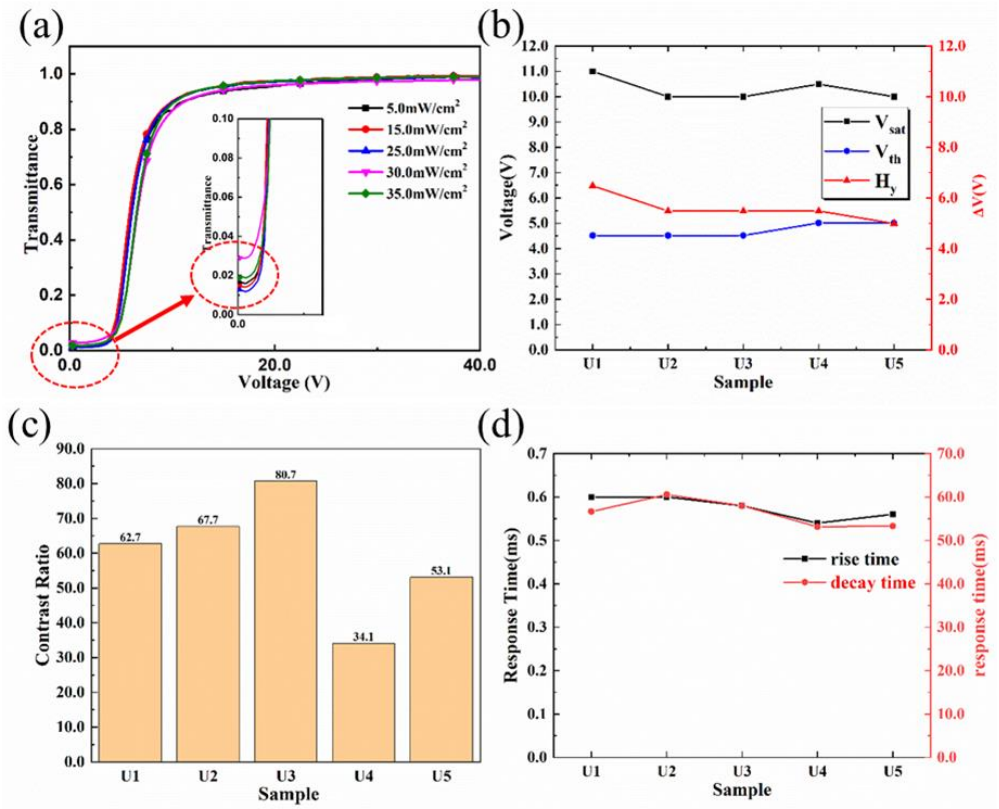
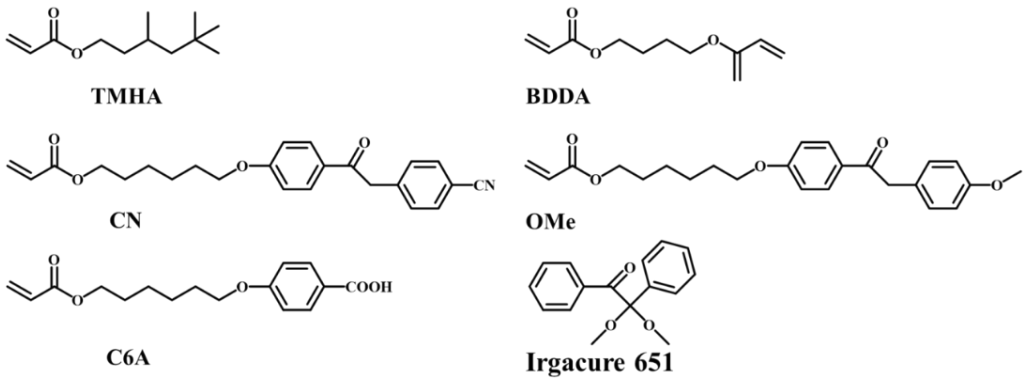


Figure 2. Electro-optical performance curves of PDLC devices under different UV intensity. (**a**) Voltage–transmittance curves from 5 mW/cm^2 to 35 mW/cm^2; (**b**) threshold voltages, saturation voltages and difference between them from Sample U1 to Sample U5; (**c**) contrast ratios from Sample U1 to Sample U5; (**d**) rise times and decay times from Sample U1 to Sample U5.

3.2. Research on the Electro-Optical Performance and Micro-Structures of PDLC Films Doped with LCMs

Three types of liquid crystalline polymerizable monomers with mono-acrylate and different functional groups were doped onto PDLC films, respectively, the molecular structure of which are shown in Scheme 1. The schematic diagram of the preparation process and working principle of PDLCs doped with LCMs is shown in Figure 3. To study the effect of the LCM on the PDLCs, three groups of samples were prepared with the composition shown in Table S1 in Supplementary Materials.



Scheme 1. Chemical structures of the materials used in this study.

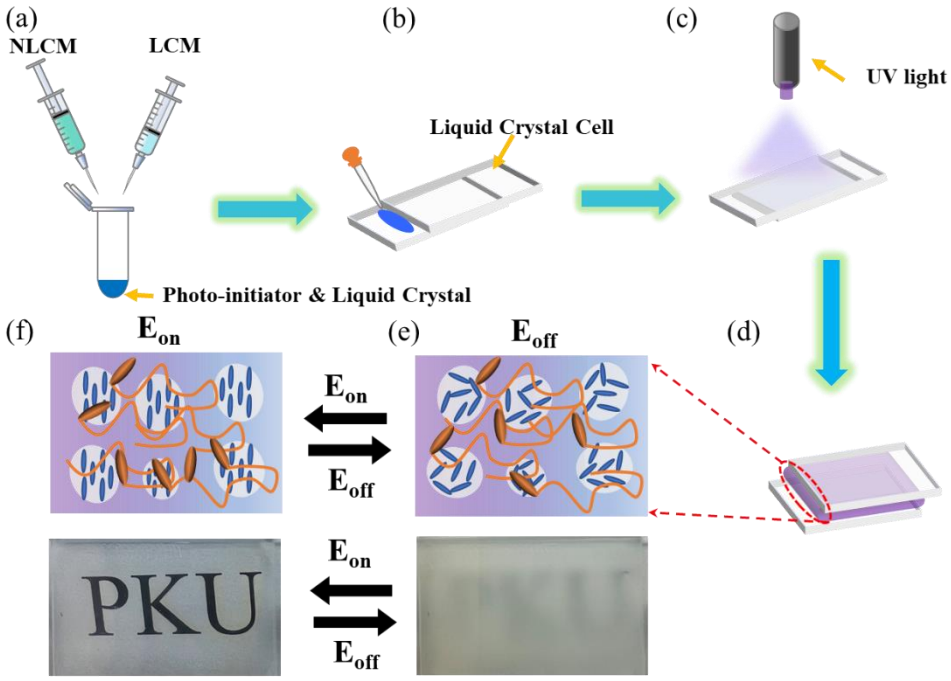


Figure 3. The schematic diagram of the preparation process and working principle of PDLCs doped with LCMs. (**a**) NLCM, LCM, photo-initiator, and liquid crystals were mixed into the burette; (**b**) the mixture was filled into a LC cell with 20 μm gap; (**c**) the LC cell was placed under a UV lamp and irradiated by 360 nm UV light with the intensity of 25.0 mW/cm^2 at ambient temperature; (**d**) after photopolymerization, the PDLC device doped with LCM was prepared; (**e**) the schematic representation of the molecular arrangement and photographs of the PDLC device without external applied electric fields; (**f**) the schematic representation of the molecular arrangement and photographs of the PDLC device with external applied electric fields.

The PDLC films doped with LCM with cyano group (denoted as CN) was prepared according to the procedures discussed above. Different contents of CN were doped into the PDLC system ranging from 1.0 wt% to 5.0 wt%. The electro-optical performance results of PDLC devices (Figure 4) indicated that the electro-optical properties of PDLC devices with different CN content have three distinct characteristics. That is, when CN content was between 1.0 wt% and 2.0 wt%, the initial transmittance of Sample N1-1 and N2-1 was rather lower than 10%. When the cyano-monomer content was between 2.0 wt% and 4.0 wt%, the initial transmittance of Sample N3-1 and N4-1 was 15%, double that of Sample N1-1 and N2-1. What is quite different from the other four samples was Sample N5-1, the PDLC device with a CN content of 5.0 wt%, whose initial transmittance was as high as 0.4. In Figure S2, when the electric field was on, obvious differences on initial transmittance can be seen in cyano PDLC devices. Concerning driving voltage curves of cyano PDLC devices, the differences between V_{th} and V_{sat} of Sample N1-1 to Sample N4-1 were within 10.0%, while compared with other four samples, V_{th} of Sample N5-1 decreased by over 50.0% to less than 10.0 V. In contrast ratio curves, like initial transmittance, the contrasts of these five components still have three different traits. The contrasts of samples with cyano monomer content between 1.0 wt% and 2.0 wt% were 200% higher than samples with cyano monomer content between 2.0 wt% and 4.0 wt%. Contrast reduction of the sample with cyano monomer content of 5.0 wt% was very obvious. The contrast of the sample with cyano monomer content of 5.0 wt% was 2.7. In curves about response time, response time was gradually shortened with the increase in cyano content. Rise time decreased from 165.0 s to 155.0 s, while decay time fell from 165.0 s to 137.5 s.

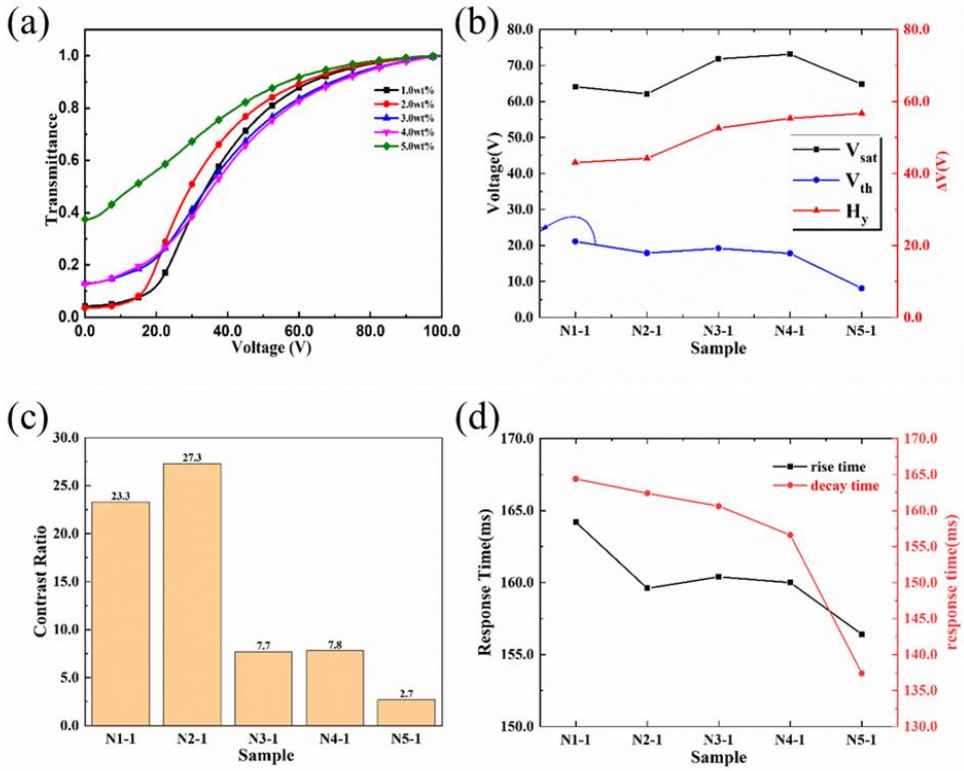


Figure 4. Electro-optical curves of PDLC devices with different cyano monomer content. (**a**) Voltage–transmittance curves from 1.0 wt% to 5.0 wt%; (**b**) threshold voltages, saturation voltages and differences between them from Sample N1-1 to Sample N5-1; (**c**) contrast ratios from Sample N1-1 to Sample N5-1; (**d**) rise times and decay times from Sample N1-1 to Sample N5-1.

In order to further investigate dependence of CN content on the micro-structures as well as electro-optical properties of cyano PDLCs, the samples of cyano PDLC devices were characterized by scanning electron microscope (SEM) and their diameters were analyzed, as shown in Figure 5. Compared with the samples without cyano monomer, the polymer network morphology of all cyano PDLC devices was a regular grid-network with an obvious topological structure. This phenomenon indicates that even if LC photopolymerizable monomers were added, they can co-product free radical polymerization of acrylate together with the NLC photopolymerizable monomers, which meant separate polymerization did not occur and LCM formed part of the matrix. The generating rate of all polymer networks is consistent, resulting in a stable and orderly morphology. When a small number of cyano monomers was introduced, the average mesh diameter of the polymer network became larger and the pore size of the polymer network became larger. The reason contributed to this phenomenon is the reduction in acrylate molar content in the PDLC films with cyano LC monomers [29]. However, along with the increase in cyano monomer content, the pore size of polymer network decreased gradually, and the size difference of each pore in the polymer network also decreased gradually. We can learn from SEM images and electro-optical performance curves that, when the cyano monomer content was between 0 wt% and 4.0 wt%, the pore size became bigger, but resulting in higher V_{th}. As LC molecules are influenced by polymer interface groups, and the force exerted on LC molecules from cyano groups is strong, it is difficult for molecules to deflect after applying the electric field. Since both polymer networks and LC molecules contain cyano groups, the strong force among molecules made it hard for cyano molecules to diffuse. In this way, the pore size was becoming smaller and smaller with the content of cyano monomer in polymer network increasing, and the cyano groups became more abundant resulting in an increase in threshold voltage. However, it was different when the content of cyano monomer was 5.0 wt%. A clear difference happened in the pore size of the

polymer network, whose diameter was increased by an order of magnitude, from several micro-meters to several tens of micro-meters. Moreover, many small holes with a diameter of several micro-meters were generated around the large holes. In comparison with the electro-optical properties of other samples, it can be known that when the content of cyano monomer was increased to 5.0 wt%, due to the increase in cyano monomer content, the content of double bonds in the PDLC film decreased, which resulted in the decrease in the amount of polymerization reaction between molecules, leading to the increase in pore size and the decrease in threshold voltage.

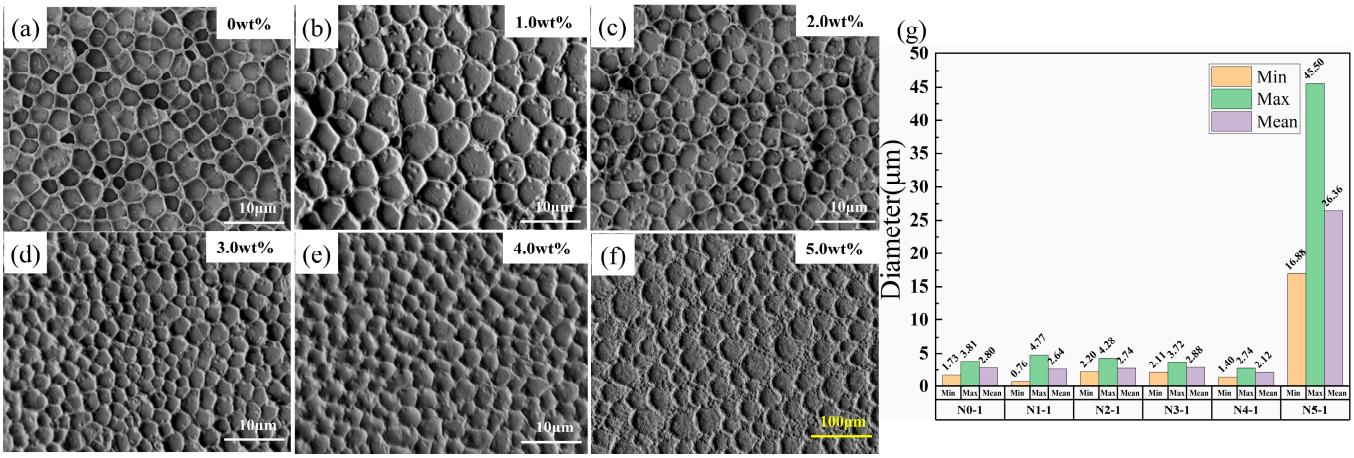


Figure 5. Top-view SEM images and pore size histogram of the PDLC films doped with the cyano LCM. SEM images of PDLC films prepared with different LCM content: (**a**) 0 wt%, (**b**) 1.0 wt%, (**c**) 2.0 wt%, (**d**) 3.0 wt%, (**e**) 4.0 wt%, (**f**) 5.0 wt%; (**g**) pore size of the PDLC films.

The PDLC films doped with LCM with methoxyl group (denoted as OMe) was prepared according to the procedures discuss above. Different content of OMe was doped into the PDLC system ranging from 1.0 wt% to 5.0 wt%. The electro-optical performance of methoxyl PDLC devices was shown in Figure 6 and their images were shown in Figure S3. The transmittance curve in Figure 6a demonstrated the change in initial transmittance. In this curve, the initial transmittance of Sample C1 with the methoxyl content of 1.0 wt% was the lowest. With the methoxyl LCM content increasing, the initial transmittance also was rising, making Sample C5 with the methoxyl content of 5.0 wt% the highest, which was 19%. The trend of V_{th} and V_{sat} was similar with the increase in methoxyl monomer content. Compared with Sample C1, whose methoxyl monomer content was 1.0 wt%, V_{th} and V_{sat} of Sample C2 with the methoxyl monomer content of 2.0 wt% have increased by nearly 100%, from 11.0 V to 21.0 V. There was basically no change in V_{th} and V_{sat} among the samples with methoxyl content ranging from 2.0 wt% to 5.0 wt%. With respect to contrast ratio and response time, the values of them decrease along with the increase in methoxyl content.

When observing the SEM images and diameter analysis of methoxyl PDLC devices (Figure 7), it can be found that its network morphology was basically in accordance with that of cyano PDLC, in the forming of a honeycomb polymer network. After doping methoxyl monomer into the PDLC device, the pore size of its polymer network was getting bigger, with the topology similar with PDLCs without LCMs. As the content of methoxyl monomer increased, the morphology of the polymer network also changed. That is, the pore size gradually reduced and the topology of the polymer network became unstable. When the content of methoxy monomer reached 5.0 wt%, the pore size reached its smallest size and the morphology of each pore was quite different. This phenomenon of methoxyl PDLCs might origin from the following reasons. The molecular structure of methoxyl LCM was similar to some components of LC mixtures, both of which contain the structure of double benzene rings. So LC methoxyl monomer had better compatibility with LC mixture, making it harder for free radicals to diffuse in photopolymerization, which made it difficult for methoxyl monomer and NLC monomer to co-polymerize. As a polar group, methoxyl

monomer made it more untoward for free radicals to diffuse. Effects of these two factors on a methoxyl PDLC film result in the phenomenon that the morphology of the polymer network becomes unstable with the increase in methoxyl monomer content. This further influences both V_{th} and V_{sat}, which leads to poor electro-optical performance.

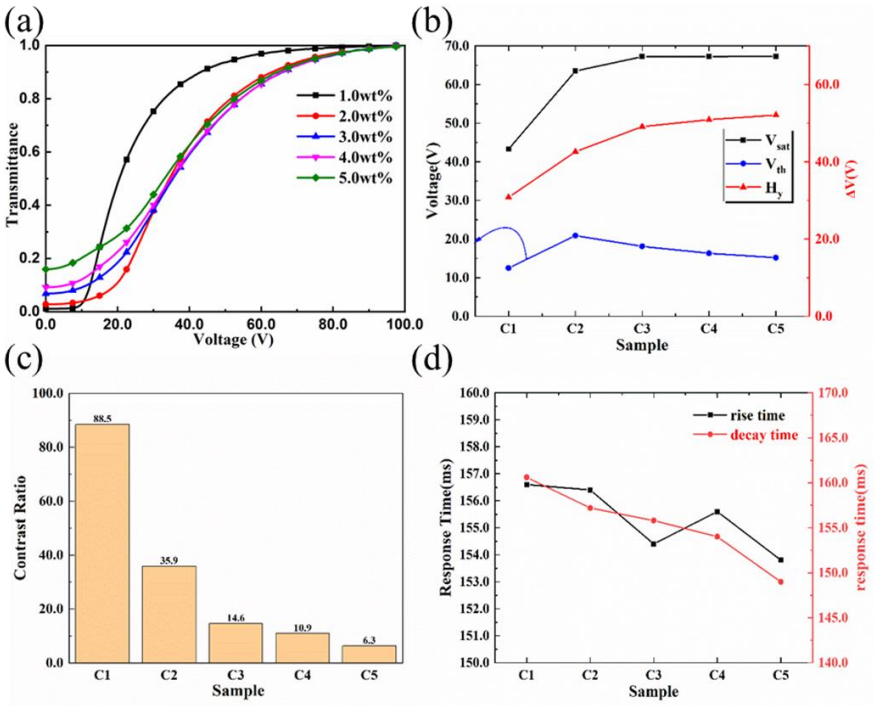


Figure 6. Electro-optical curves of PDLC devices with different methoxyl monomer content from 1.0 wt% to 5.0 wt%. (**a**) Voltage-transmittance curves from 1.0 wt% to 5.0 wt%; (**b**) Threshold voltages, saturation voltages and differences between them from Sample C1 to Sample C5; (**c**) Contrast ratios from Sample C1 to Sample C5; (**d**) Rise times and decay times from Sample C1 to Sample C5.

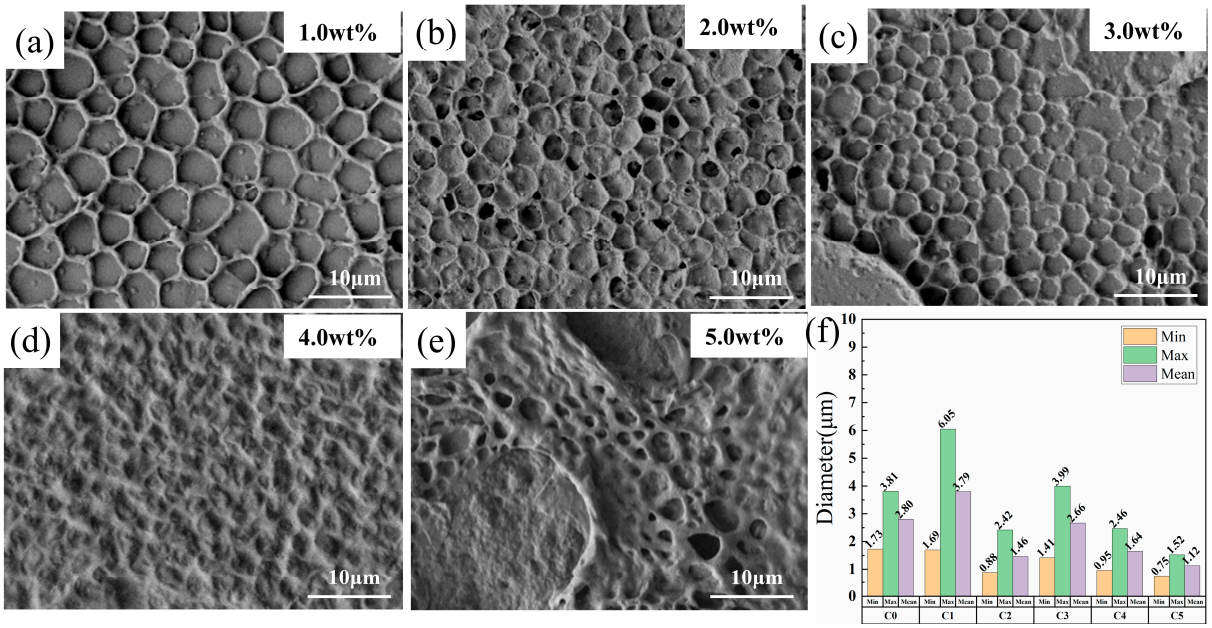


Figure 7. Top-view SEM images and pore size histogram of the PDLC films prepared with the methoxyl monomer. SEM images of PDLC films prepared with different LCM content: (**a**) 1.0 wt%, (**b**) 2.0 wt%, (**c**) 3.0 wt%, (**d**) 4.0 wt%, (**e**) 5.0 wt%, (**f**) Pore-size of the PDLC films.

The PDLC films doped with LCM with carboxyl group (denoted as C6A) was prepared according to the procedures discuss above. Different content of C6A was doped into the PDLC system ranging from 1.0 wt% to 5.0 wt%. The electro-optical properties of the carboxyl PDLC film was characterized which shown significant features different from PDLCs doped with CN or OMe (shown in Figure 8). First of all, in the transmittance curve (Figure 8a), the initial transmittance of each component sample was basically the same (the images of carboxyl PDLC films were shown in Figure S4). What is more, on the curves of driving voltage, contrast ratio and response time, taking the carboxyl monomer content of 2.0 wt% as the dividing line, obvious differences happen in the electro-optical properties of the carboxyl PDLC film. When the content of carboxyl monomer content was lesser than or equal to 2.0 wt% (shown as Sample A1 and Sample A2), both V_{th} and V_{sat} maintained at a lower level, with their V_{th} at around 10.0 V, contrast ratio over 100 and a faster response time. When the content of carboxyl monomer content was larger than 2.0 wt% (Sample A3, Sample A4, and Sample A5), threshold voltage had been greatly improved, which was doubled to 20.0 V. The contrast ratio decreased by over 50% and the response time increased. It suggests that the electro-optical performance of PDLC films with carboxyl monomer content over 2.0 wt% deteriorate sharply.

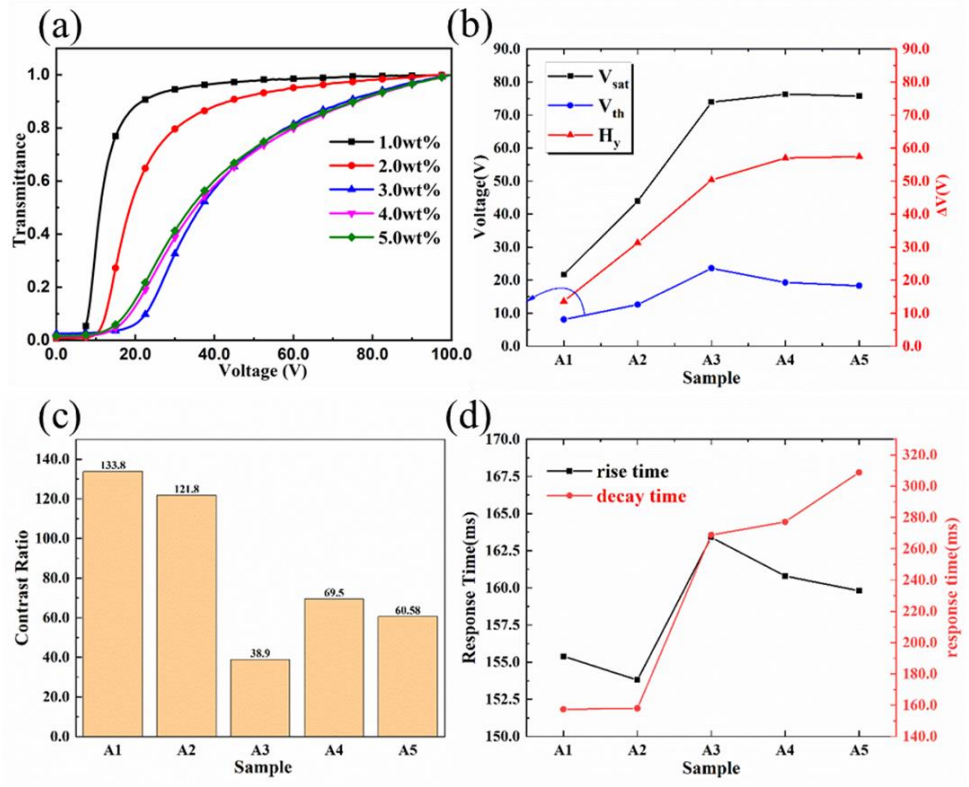


Figure 8. Electro-optical curves of PDLC devices with different carboxyl monomer content from 1.0 wt% to 5.0 wt%. (**a**) Voltage-transmittance curves from 1.0 wt% to 5.0 wt%; (**b**) Threshold voltages, saturation voltages and differences between them from Sample A1 to Sample A5; (**c**) Contrast ratios from Sample A1 to Sample A5; (**d**) Rise times and decay times from Sample A1 to Sample A5.

From the SEM images and diameter analysis of carboxyl PDLC films (shown in Figure 9), it can be seen that the pore size became larger when carboxyl monomer was doped at the beginning. Like cyano PDLC films and methoxyl PDLC films, in every 100.0 g polymer of a PDLC film, the content of acrylate double bonds ranged from only 0.1211 mol of NLCM PDLC device to 0.1183 mol of carboxyl PDLC device. With the decrease in the molar content of double bonds, the pore size of carboxyl PDLC polymer network increased. Unlike cyano PDLC films and methoxyl PDLC films, the topology of carboxyl PDLC films' network was destructed. The morphology of pores began to appear irregular, which was mainly

characterized by its large size span and increased turbidity. This became increasingly obvious with the increase in carboxyl monomer content. When the carboxyl monomer content was over 2.0 wt%, with the increase in carboxyl monomer content, the pore size of polymer network decreased. The morphology of its polymer network gradually changed from honeycomb to micropore, and it no longer had topological structure. This indicated once again that when the carboxyl content was more than 2.0 wt%, the electro-optical properties of PDLCs become worse, which was mainly demonstrated by an increase in V_{th} and a decrease in contrast ratio. The main reason responsible for this phenomenon was that carboxyl monomers had hydrogen bonds in their molecules, so the interaction between molecules affects the morphology of its polymer network. Particularly, the influence of intermolecular interaction was increasing with the increase in carboxyl monomer content. The arrangement of molecules interfering with photopolymerization free radicals' reaction lead to the morphology of its polymer network gradually changing from the previous topology to disordered and chaotic structure. Consequently, the pore size becomes very small.

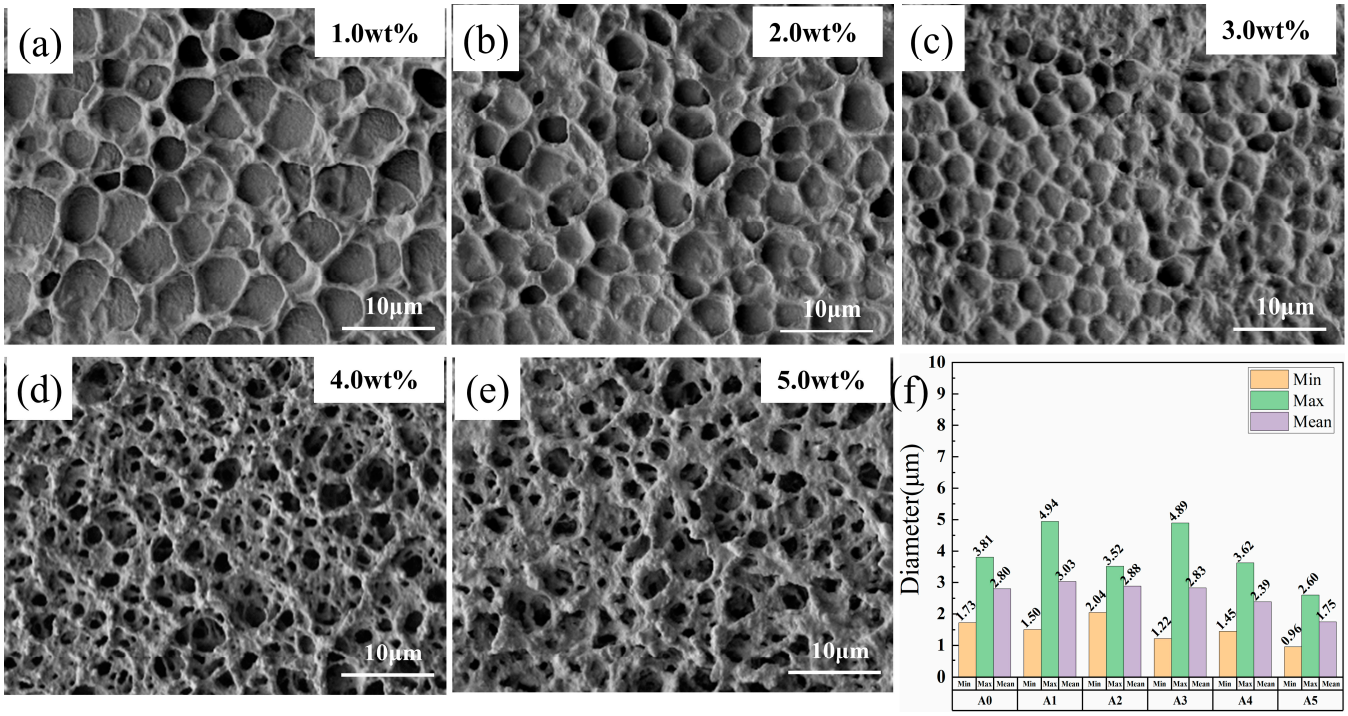


Figure 9. Top-view SEM images and pore size histogram of the PDLC films prepared with the carboxyl monomer. SEM images of PDLC films prepared with different LCM content: (**a**) 1.0 wt%, (**b**) 2.0 wt%, (**c**) 3.0 wt%, (**d**) 4.0 wt%, (**e**) 5.0 wt%, (**f**) Pore-size of the PDLC films.

4. Conclusions

In conclusion, the influence of LCMs with acrylate end-group and different functional groups on the micro-structures and electro-optical performance of PDLC films were systematically studied. Results show that low content doping (ca. 1.0 wt%) of LCM would induce enlarged pore size due to the decreased molar content of acrylate group. The driving voltages of the PDLC films were affected by the functional group of the LCM. The functional group of LCM with high polarity would greatly increase the driving voltage. With the increase in the doping content of LCMs, the pore size of the PDLC films became smaller due to increased difficulties for free radicals to diffuse, which result from the good compatibility of these three LCMs with small molecular LCs. Interestingly, when the doping content of LCM with cyano-group reached 5.0 wt%, the pore size of the PDLC films abruptly became larger and the driving voltage decreased on the account of the reduction in the amount of polymerization reaction between molecules, stemming from the diminution in

the content of double bonds. This study is aimed at providing novel views for optimizing the electro-optical performance of PDLC films containing LCMs and might provide some guidelines for the study of novel PDLCs.

Supplementary Materials: The following supporting information can be downloaded at: https://www.mdpi.com/article/10.3390/cryst13091294/s1, Figure S1: Crystallization situations of samples under the polarization microscope with the temperature of (a) 5.0 °C, (b) 15.0 °C, (c) 25.0 °C, (d) 30.0 °C, (e) 35.0 °C; Table S1:Composition ratios of the LC 1717, THMA, BDDA and liquid crystalline monomers for PDLC devices; Figure S2: Images of PDLC devices doped with cyano LC monomers at off-state and on-state (applied volt-age: 100 V); Figure S3: Images of PDLC devices doped with methoxyl LC monomers at off-state and on-state (applied voltage: 100 V); Figure S4: Images of PDLC devices doped with carboxyl LC monomers at off-state and on-state (applied voltage: 100 V).

Author Contributions: Conceptualization, C.M., C.Z. and H.Y.; methodology, C.M. and M.Y.; validation, C.M.; formal analysis, C.M., Y.G. and Y.W.; investigation, J.X.; resources, J.X., C.Z. and C.M.; data curation, C.M.; writing—original draft preparation, C.M.; writing—review and editing, C.Z.; visualization, Y.G.; supervision, C.Z. and H.Y.; project administration, C.Z. and H.Y.; funding acquisition, J.X. and C.Z. All authors have read and agreed to the published version of the manuscript.

Funding: This research was funded by the National Natural Science Foundation of China (Grant No. 52073028, 52203322).

Data Availability Statement: The data supporting the findings of the study are available from the corresponding authors upon reasonable request.

Conflicts of Interest: The authors declare no conflict of interest.

References

1. Jelle, B.P.; Hynd, A.; Gustavsen, A. Fenestration of today and tomorrow: A state-of-the-art review and future research opportunities. *Sol. Energy Mater. Sol. Cells* **2012**, *96*, 1–28. [CrossRef]
2. Bronnikov, S.; Kostromin, S.; Zuev, V. Polymer-dispersed liquid crystals: Progress in preparation, investigation, and application. *J. Macromol. Sci.* **2013**, *52*, 1718–1735. [CrossRef]
3. Li, K.; Wang, J.; Cai, W.; He, H.; Cen, M.; Liu, J.; Luo, D.; Mu, Q.; Gerard, D.; Liu, Y. Electrically switchable, polarization-sensitive encryption based on aluminum nanoaperture arrays integrated with polymer-dispersed liquid crystals. *Nano Lett.* **2021**, *21*, 7183–7190. [CrossRef]
4. Kumano, N.; Seki, T.; Ishii, M.; Nakamura, H.; Umemura, T.; Takeoka, Y. Multicolor polymer-dispersed liquid crystal. *Adv. Mater.* **2011**, *23*, 884–888. [CrossRef]
5. Shivaraja, S.J.; Gupta, R.K.; Manjuladevi, V. Faster switching polymer dispersed liquid crystal devices incorporated with functionalized SWCNTs. *J. Mol. Liq.* **2022**, *354*, 118905. [CrossRef]
6. Jiang, Z.; Zheng, J.; Liu, Y.; Zhu, Q. Investigation of dielectric properties in polymer dispersed liquid crystal films doped with CuO nanorods. *J. Mol. Liq.* **2019**, *295*, 111667. [CrossRef]
7. Hikmet, R.; Kemperman, H. Electrically switchable mirrors and optical components made from liquid crystal gels. *Nature* **1998**, *392*, 476–479. [CrossRef]
8. Hinojosa, S.C.A. Sharma, Effects of gold nanoparticles on electro-optical properties of a polymer-dispersed liquid crystal. *Appl. Phys. Lett.* **2010**, *97*, 081114. [CrossRef]
9. Doane, J.W.; Vaz, N.A.; Wu, B.G.; Žumer, S. Field controlled light scattering from nematic microdroplets. *Appl. Phys. Lett.* **1986**, *48*, 269–271. [CrossRef]
10. He, Z.; Yin, K.; Hsiang, E.; Wu, S. Volumetric light-shaping polymer-dispersed liquid crystal films for mini-LED backlights. *Liq. Cryst.* **2020**, *47*, 1458–1463. [CrossRef]
11. Liao, C.; Su, C.; Chen, M. Mitigation of image blurring for performance enhancement in transparent displays based on polymer-dispersed liquid crystal. *Displays* **2019**, *56*, 30–37. [CrossRef]
12. Katariya-Jain, A.; Deshmukh, R.R. Effects of dye doping on electro-optical, thermo-electro-optical and dielectric properties of polymer dispersed liquid crystal films. *J. Phys. Chem. Solids* **2022**, *160*, 110363. [CrossRef]
13. Sharma, V.; Kumar, P. Electro-optically oriented Kerr and orientational phase study of normal mode polymer dispersed liquid crystals-Effect of dispersion of nanoparticles. *J. Mol. Liq.* **2022**, *348*, 118030. [CrossRef]
14. Loiko, V.A.; Konkolovich, A.V.; Miskevich, A.A.; Manaila-Maximean, D.; Danila, O.; Cîrcu, V.; Bărar, A. Optical model to describe coherent transmittance of polymer dispersed liquid crystal film doped with carbon nanotubes. *J. Quant. Spectrosc. Radiat. Transf.* **2020**, *245*, 106892. [CrossRef]

15. Sun, Y.; Zhang, C.; Zhou, L. Effect of a polymercaptan material on the electro-optical properties of polymer-dispersed liquid crystal films. *Molecules* **2016**, *22*, 43. [CrossRef] [PubMed]
16. Ellahi, M.; Liu, F.; Song, P.; Gao, Y.; Rafique, M.Y.; Khan, D.F.; Cao, H.; Yang, H. Characterization and morphology of polymer-dispersed liquid crystal films. *Soft Mater.* **2014**, *12*, 339–345. [CrossRef]
17. Yang, D.K.; Wu, S.T. *Fundamentals of Liquid Crystal Devices*; John Wiley & Sons: Hoboken, NJ, USA, 2014.
18. Jia, M.; Zhao, Y.; Gao, H. High dielectric properties, TiO_2 nanoparticles doped PDLC devices for lower switching voltage. *Liq. Cryst.* **2022**, *49*, 333–342. [CrossRef]
19. Yu, M.; Xu, J.; Luo, L. Role of Hydroxy Group in the Electro-Optical Properties of Polymer-Dispersed Liquid Crystals. *Crystals* **2023**, *13*, 843. [CrossRef]
20. Zhang, P.; Tong, X.; Gao, Y. A Sensing and Stretchable Polymer-Dispersed Liquid Crystal Device Based on Spiderweb-Inspired Silver Nanowires-Micromesh Transparent Electrode. *Adv. Funct. Mater.* **2023**, *online version of record*. [CrossRef]
21. Jamil, M.; Ahmad, F.; Rhee, J.T.; Jeon, Y.J. Nanoparticle-doped polymer-dispersed liquid crystal display. *Curr. Sci.* **2011**, *101*, 1544–1552.
22. Kizhakidathazhath, R.; Nishikawa, H.; Okumura, Y. High-performance polymer dispersed liquid crystal enabled by uniquely designed acrylate monomer. *Polymers* **2020**, *12*, 1625. [CrossRef]
23. Ghosh, A. Investigation of vacuum-integrated switchable polymer dispersed liquid crystal glazing for smart window application for less energy-hungry building. *Energy* **2023**, *265*, 126396. [CrossRef]
24. Bobnar, M.; Derets, N.; Umerova, S. Polymer-dispersed liquid crystal elastomers as moldable shape-programmable material. *Nat. Commun.* **2023**, *14*, 764. [CrossRef] [PubMed]
25. Liang, X.; Guo, S.; Chen, M. A temperature and electric field-responsive flexible smart film with full broadband optical modulation. *Mater. Horiz.* **2017**, *4*, 878–884. [CrossRef]
26. Guo, S.; Liang, X.; Zhang, H. An electrically light-transmittance-controllable film with a low-driving voltage from a coexistent system of polymer-dispersed and polymer-stabilised cholesteric liquid crystals. *Liq. Cryst.* **2018**, *45*, 1854–1860. [CrossRef]
27. Liang, X.; Guo, C.; Chen, M. A roll-to-roll process for multi-responsive soft-matter composite films containing Cs_xWO_3 nanorods for energy-efficient smart window applications. *Nanoscale Horiz.* **2017**, *2*, 319–325. [CrossRef] [PubMed]
28. Liang, X.; Chen, M.; Guo, S. Programmable electro-optical performances in a dual-frequency liquid crystals/polymer composite system. *Polymer* **2018**, *149*, 164–168. [CrossRef]
29. Baars, M.W.P.L.; van Boxtel, M.C.W.; Bastiaansen, C.W.M. A Scattering Electro-Optical Switch Based on Dendrimers Dispersed in Liquid Crystals. *Adv. Mater.* **2000**, *12*, 715–719. [CrossRef]

Disclaimer/Publisher's Note: The statements, opinions and data contained in all publications are solely those of the individual author(s) and contributor(s) and not of MDPI and/or the editor(s). MDPI and/or the editor(s) disclaim responsibility for any injury to people or property resulting from any ideas, methods, instructions or products referred to in the content.